Journal of Biomechanical Science and Engineering

Vol. 2, No. 3, 2007

Mechanical Characterization of Brain Tissue in High-Rate Compression*

Atsutaka TAMURA**, ***, Sadayuki HAYASHI***, Isao WATANABE***, Kazuaki NAGAYAMA** and Takeo MATSUMOTO**

**Nagoya Institute of Technology,
Gokiso-cho Showa-ku, Nagoya 466-8555, Japan
***Toyota Central R&D labs., Inc.,
Yokomichi Nagakute, Aichi-gun 480-1192, Japan
E-mail: a-tamura@mosk.tytlabs.co.jp

Abstract

Mechanical properties of brain tissue in high strain region are indispensable for the analysis of brain damage during traffic accidents. However, accurate data on the mechanical behavior of brain tissue under impact loading condition are sparse. In this study, mechanical properties of porcine brain tissues were characterized in their cylindrical samples cored out from their surface. The samples were compressed in their axial direction at strain rates ranging from 1 to 50 s^{-1}. Stress relaxation test was also conducted following rapid compression with a rise time of ~30 ms to different strain levels (20-70%). Brain tissue exhibited stiffer responses under higher impact rates: initial elastic modulus was 5.7±1.6, 11.9±3.3, 23.8±10.5 kPa (mean±SD) for strain rate of 1, 10, 50 s^{-1}, respectively. We found that stress relaxation $K(t,\varepsilon)$ could be analysed in time and strain domains separately. The relaxation response could be expressed as the product of two mutually independent functions of time and strain as: $K(t,\varepsilon) = G(t)\sigma^e(\varepsilon)$, where $\sigma^e(\varepsilon)$ is an elastic response, i.e., the peak stress in response to a step input of strain ε, and $G(t)$ is a reduced relaxation function: $G(t) = 0.642e^{-t/0.0207} + 0.142e^{-t/0.482} + 0.216e^{-t/18.9}$, i.e., the time-dependent stress response normalized by the peak stress. The reduced relaxation function obtained here will serve as a useful tool to predict mechanical behavior of brain tissue in compression with strain rate greater than 10 s^{-1}.

Key words: Brain Tissue, Viscoelasticity, Stress, Strain, High-Rate Compression, Relaxation

1. Introduction

The head has been identified as the body region most frequently involved in life-threatening injuries in traffic accidents. In particular, intracranial brain deformation caused by rapid head rotation or blunt impact to the head during injurious events is regarded as responsible for traumatic brain injuries (TBIs) such as acute subdural hematoma, brain contusion, and diffuse axonal injury. To estimate the incidence of these internal wounds, their injury mechanism has to be revealed in detail so that effective brain injury criteria can be derived, which may lead to the installation of promising countermeasures against TBI. In recent years, several research groups introduced experimentally verified mathematical models for human head to study injury mechanisms of TBI [1, 2]. For such models, the description of precise constitutive behavior of brain tissue is crucial to improve the validity of these models for better injury prediction.

Over the past several decades, a number of research groups have focused on the mechanical properties of brain tissue in order to establish constitutive relationships over a wide range of loading conditions. Most of them conducted oscillatory dynamic shear deformation tests in the frequency range of 0.1 to 10000 Hz [3-9] while others performed compressive or tensile tests applied at moderate loading rates below ~1 s^{-1} [10-14]. Since

*Received 24 Apr., 2007 (No. 07-0200)
[DOI: 10.1299/jbse.2.115]

biological soft tissues are nonlinear viscoelastic material in nature, mechanical behavior of brain tissue may be modeled in different ways based on the specific conditions of interest and magnitude of the strain rate [15]. In fact, a typical head impact injury event has a duration on the order of milliseconds. Thus, as for impact situations related to TBI, we need to characterize tissue properties over the expected range of loading rate appropriate for potentially injurious circumstances. Previous studies suggested that TBI occurs due to large strain greater than ~0.2 applied at high strain rate greater than 10 s^{-1} [16-18]. As a first step, therefore, we developed a test apparatus to investigate mechanical properties of brain tissue in high-rate compression over this range and stress relaxation response that follows the compression. This work was designed to give more insight into the tissue behavior under the environment that is typical for an injury producing event.

2. Materials and Methods

2.1 Specimen preparation

Brain tissue consists of gray and white matters and is covered with the pia and arachnoid membranes. While the gray matter is composed of an accumulation of cell bodies that do not seem to have directional preference, the white matter is formed by a bundle of neural fiber arrangements that can be highly oriented [9]. In general, some regions of the white matter can be considered as a transversely isotropic structure whilst the gray matter is simply isotropic [19, 7]. Thus, we need to make anatomical location and excised orientation of specimens remained consistent to diminish the potential effect of material anisotropy and heterogeneity.

Specimens were prepared according to Miller and Chinzei [10] with a slight modification. Fresh brains were obtained from six-month old pigs at a local slaughter house immediately after death, kept in an iced cooler box, and transported to our laboratory within 0.5 hour. Cylindrical specimens were then cored out from the corona radiata and the cerebral cortex in both the superior-inferior and the medial-lateral directions by using a steel pipe with inner diameter of 23 mm whose inner wall had been electropolished at one end to sharpen the edge like a blade. Subsequently, the specimens were cut with a surgical scalpel at the white matter end to make them about 14 mm long. Prior to dissection, each of the brains was stored in a freezer for 1 h to make a thin layer of the cerebral cortex on the specimen surface (approximately ~2-3 mm in depth) partially but not completely frozen like a sherbet. By doing so, the pia mater became stiff enough to be cut by the edge of the steel pipe with minimal tissue distortion. In most cases, two samples were taken from the anterior and posterior portions of each hemisphere for each porcine brain. Consequently, four cylindrical samples with a diameter of ~22 mm and a length of ~14 mm were harvested from each brain. The actual diameter and height of the unloaded specimens were 22.1±0.1 mm and 14.2±0.2 mm (mean±SEM, n=109), respectively, and were statistically the same among experimental groups used in this series of experiments. The samples were placed in a covered Petri dish and stored in a refrigerator until the mechanical test to prevent dehydration.

2.2 Test apparatus

Unconfined compression tests were performed in a test apparatus as shown in Figure 1. A cylindrical specimen was compressed in its axial direction by a platen connected to a crosshead of the tester. The crosshead was driven downward by a programmable linear actuator (F20-20BK-11, Yamaha), whose maximum velocity was about 1200 mm/s. A load cell (LUR-A-50NSA1, Kyowa) with measurement range of -50 to +50 N was attached under the specimen stage. The crosshead was connected with the actuator via a magnet. Once it hit the stoppers and the tensile load between the crosshead and the actuator exceeded 40 N, the crosshead detached from the actuator to prevent the damage of the load cell due to overload. To know the instant of contact between the platen and the specimen, a strip of metal tape was applied to the surface of the platen and the specimen stage. A contact signal indicating the conduction between the tapes was used as the trigger of the onset of a high-speed camera recording (Memrecam Ci-3-J, NAC). The recorded images were used to ensure that each sample was uniformly expanded between the upper platen and the specimen stage during compression. Axial position of the crosshead was measured

using a laser displacement meter (LDM) (LK-G85, Keyence) while specimen diameter was measured at the middle section of the specimen using a laser-sheet type radial displacement meter (LS-7070, Keyence). The initial diameter was used to obtain the initial cross-sectional area of each sample. This measurement setup was also used to determine zero strain point in stress-strain responses as is explained in Section 2.4. All data were recorded through A/D converter (ADA16-32/2(CB)F, Contec). Prior to A/D conversion, axial force applied to the specimen (Ch1) was amplified by a strain amplifier (SA-100D, TEAC), and all signals but trigger (Ch2) were filtered by a 1-kHz low-pass filter (Multichannel SR filter 3315, NF). Specimens were not preconditioned due to its inherent nature of delicacy and adhesiveness [10, 13]. Only one loading cycle was applied for each sample.

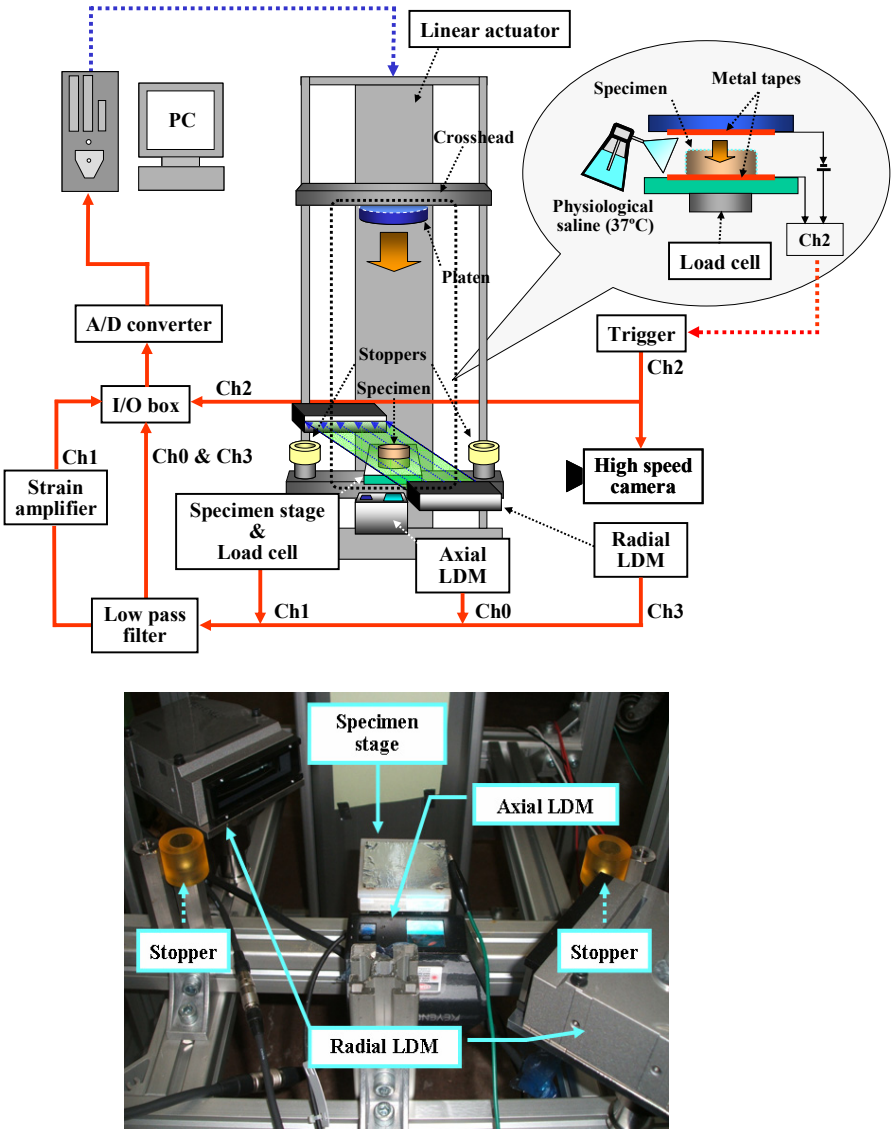

Figure 1: Schematic diagram of the test apparatus (top) and photograph of the measurement section (bottom) for high-rate compression.

2.3 Compression test

A series of unconfined compression tests were carried out at three loading rates. The velocity of the crosshead was set at 12 mm/s, 120 mm/s, and 600 mm/s, that correspond approximately to strain rates of 1, 10, and 50 s^{-1}, respectively. To ensure a pure slip boundary between the specimen and the apparatus and to keep the specimen wet, the upper and bottom surfaces of each specimen were fully lubricated by spraying warmed physiological saline (37°C), and the effective slip condition was confirmed photographically by visual inspection. The test was conducted at room temperature ~20°C.

Apart from examination of strain rate sensitivity of brain tissue, three factors were considered: effects of anatomical location, excised orientation, and specimen freezing. First, specimens were obtained in the superior-inferior direction from two different anatomical locations, i.e., anterior portion (n=20) and posterior portion (n=15). To check regional heterogeneity of brain tissue, stress-strain relationships at strain rates of 1, 10, and 50 s^{-1} were compared between specimens excised from anterior portion (n=5, 8, 7) and those excised from posterior portion (n=4, 5, 6). Second, additional specimens were obtained in the medial-lateral direction (n=13). To check the effects of specimen orientation, their stress-strain relationship was measured at the rate of 1 s^{-1} and compared with the specimens cored out in the superior-inferior direction (n=9) with no distinction between anatomical locations. In addition, an effect of specimen freezing was examined. For this purpose, specimens obtained from non-frozen brain in the superior-inferior direction (n=11) were compressed at the rate of 1 s^{-1}, and their mechanical response was compared with that of frozen specimens (n=9). The strain rate sensitivity of brain tissue was examined in the stress-strain relationships obtained in the first experiment. The number of specimens used in the rate sensitivity test was summarized in Table 1.

Table 1: Loading rate, sample location, and sampling interval for the rate sensitivity test.

Velocity (mm/s)	Strain rate (s^{-1})	n (N=12) A	n (N=12) P	Sampling interval (μs/ch)
12	1	5	4	500
120	10	8	5	250
600	50	7	6	250

A, anterior portion; P, posterior portion; n, number of samples; N, number of brains.

2.4 Definition of stress and strain

Zero strain point was defined referring to diameter change detected by the radial LDM [10]. Due to high compliance of the vibration of the tester, it was difficult to determine the zero strain point with load cell signal. An analysis with a high-speed video camera showed that the load cell signal increased significantly from zero level when the specimen was compressed by ~2 mm, and concomitant radial displacement was 0.25 mm for 1 s^{-1} and 10 s^{-1} compression and 0.03 mm for 50 s^{-1} compression. Thus, the zero strain point was defined as the point when the increase in diameter reached these values. In this experimental setup, undeformed height of the specimen might be determined by the gap between the upper and lower platens when the upper platen came into contact with the upper surface of the specimen. However, the onset of the contact signal did not correspond to the onset of specimen deformation due to the variation of the specimen surface hydration. Thereby, the height of the specimen at thus defined zero strain point was used as the initial dimension of the specimen to calculate nominal strain. Nominal stress was calculated based on the axial force and initial cross-sectional area of each sample. We also obtained apparent elastic moduli E_1, E_2, and E_3 as the slope of the stress-strain curve in the strain range of 0-0.2, 0.2-0.4, and 0.4-0.5, respectively (Fig. 2).

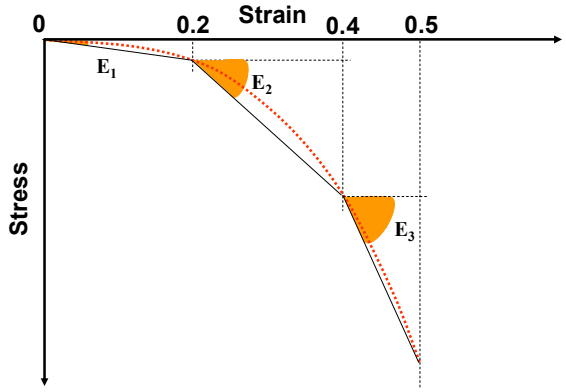

Figure 2: Definition of apparent elastic moduli of brain tissue.

2.5 Relaxation test

The relaxation experiments were conducted similarly using 50 samples obtained from 14 brains to characterize the brain tissue response to a step-like strain in the form of a stress relaxation test. Specimens were compressed at 600 mm/s (50 s^{-1}) to various strain levels and held for 8 s with the sampling rate of 2 kHz/channel. In order to investigate the potential effect of the applied strain levels, we varied the magnitude of compressive strains in the range of 15-74%. Data were then obtained at each nominal strain 20, 30, 40, 50, 60, and 70% by classifying the applied strain magnitude into six stages, i.e., 15-24 (n=6), 25-34 (n=12), 35-44 (n=11), 45-54 (n=7), 55-64 (n=7), 65-74% (n=7), respectively.

In this study, a reduced relaxation function, $G(t)$, the time-dependent stress response of the tissue at the instant immediately after the step loading, was obtained by normalizing relaxation curve by its peak force (Eq. 1), and was approximated by a sum of exponentials (Eq. 2):

$$G(t) = \frac{F(t)}{F(0+)} \quad \text{(Eq. 1)}$$

$$G(t) = G_1 e^{-t/\tau_1} + G_2 e^{-t/\tau_2} + G_3 e^{-t/\tau_3} \quad \text{(Eq. 2)}$$

where τ_1, τ_2, and τ_3 are the time constants. The coefficients for the final equation form of this reduced relaxation function was chosen such that the sum of three coefficients satisfied below condition as given in (Eq. 3), because instantaneous modulus $G(0)$ is unity.

$$G_1 + G_2 + G_3 = 1 \quad \text{(Eq. 3)}$$

Consequently, the curve fitting procedure using three exponentials produced an excellent fit both statically (R^2=0.985) and visually. Since our interest is limited to the time duration related to the impact situations, a long-term coefficient G_∞ representing the percentage of stress at the equilibrium state was not taken into account.

3. Results

3.1 Examination of methodology

3.1.1 Effect of anatomical origin and orientation of the specimen

Positional difference in the mechanical properties of the brain tissue was minor. Elastic moduli E_1, E_2, and E_3, were not significantly different between specimens obtained from anterior and posterior portions (unpaired t-test, data not shown). Data obtained from anterior and posterior portions were thus combined together for further analysis. Figure 3 summarizes stress-strain relationships obtained at the strain rate of 1 s^{-1} across different environmental conditions. As demonstrated in Figures 3a and b, direction of excision was not involved in material property either. Although they are preliminary, these results indicate that neither the anatomical origin nor orientation of the specimen affect its mechanical properties significantly in macroscopic point of view.

3.1.2 Effect of specimen freezing

Stress-strain relationships were quite similar between frozen and fresh specimens (Figs. 3a and c). There were no significant differences in elastic moduli E_1, E_2, and E_3 between frozen and fresh specimens either (unpaired t-test). In addition, stress-strain relationship of fresh porcine brain obtained by Miller and Chinzei [10] was almost similar to our result obtained at the rate of 1 s^{-1} (Fig. 3d). We thus confirmed that the effect of specimen freezing in the current study was negligible in macroscopic material responses.

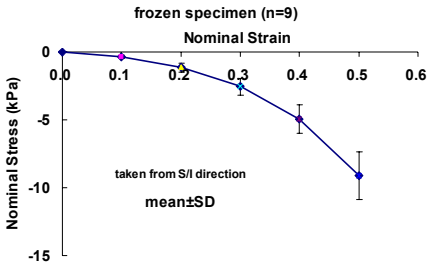

(a) Frozen specimens cored out in the superior-inferior direction.

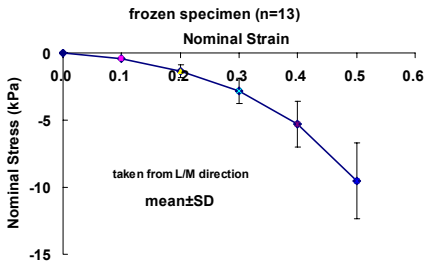

(b) Frozen specimens cored out in the medial-lateral direction.

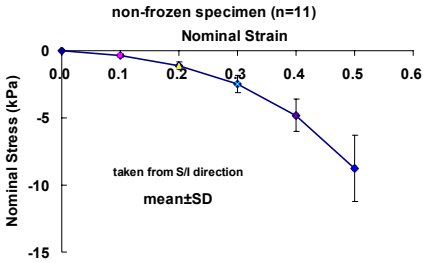

(c) Non-frozen specimens cored out in the superior-inferior direction.

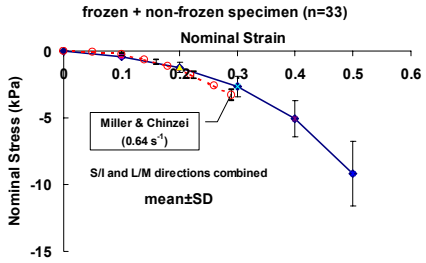

(d) Frozen and non-frozen specimens combined together.

Figure 3: Stress-strain relationships obtained at strain rate of 1 s^{-1}.

3.2 Strain-rate dependency of the mechanical properties of brain tissue

Figure 4 shows a typical example for the time course of stress and strain responses obtained at the fastest loading rate compression (50 s^{-1}). Even in the fastest compression, stress and strain could be obtained with sufficient resolution. Stress response was nonlinear with a toe region, and loading rate was almost constant. Although oscillation was observed in the stress curve, its amplitude was small enough to reveal the nonlinear mechanical properties. This oscillation was found to be different from the stress wave caused by the collision between the platen and the specimen, for the time required for the impulse wave to travel back and forth along the specimen thickness once was ~5 ms.

Stress-strain curves of the brain tissue were summarized in Figure 5. The curves were rate dependent and brain tissue stiffens noticeably with increasing strain rate. Measured elastic moduli are also summarized in Table 2. Significant difference was observed between each of the apparent elastic moduli at three different strain levels.

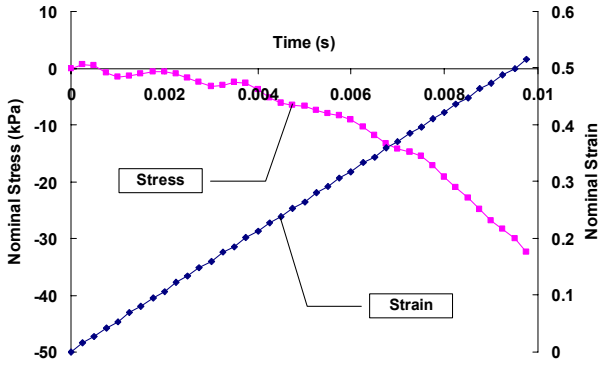

Figure 4: Typical responses obtained in high-rate compression of brain tissue.

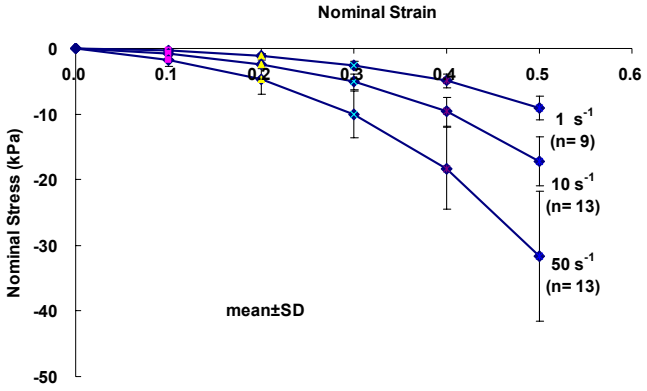

Figure 5: Averaged stress-strain relationships in unconfined compression test.

Table 2: Apparent elastic moduli of brain tissue (mean±SD).

Strain rate (s^{-1})	E_1 (kPa)	E_2 (kPa)	E_3 (kPa)
1	5.7 ± 1.6	19.0 ± 3.8	41.9 ± 8.9
10	11.9 ± 3.3*	36.4 ± 7.8*	75.3 ± 16.8*
50	23.8 ± 10.5*,**	67.6 ± 19.6*,**	133.6 ± 38.6*,**

*P<0.01 vs. 1 s^{-1}, **P<0.01 vs. 10 s^{-1}

3.3 Relaxation response

Typical strain history to a preset strain ε_0 (20-70%) and its concomitant force response of brain tissue are shown in Figures 6a and b, respectively. During stress relaxation test, the compressive force decreased very rapidly within 25 ms, then continued decreasing gradually and did not reach a plateau within the time range allowed here. The compressive force decreased by ~70% in 1 s after the load was applied. The force relaxation appeared to change as a function of applied strain (Fig. 7a). However, by normalizing the relaxation response with its peak force in each case as given in (Eq. 1), the brain tissue was found to be a strain-time separable material in the range of strains and times tested here (Fig. 7b), i.e., the stress relaxation $K(t,\varepsilon)$ could be expressed as the product of two mutually independent functions of time and strain as follows [20]:

$$K(t,\varepsilon) = G(t)\sigma^e(\varepsilon) \qquad \text{(Eq. 4)}$$

where $\sigma^e(\varepsilon)$ is an elastic response, i.e., the peak stress in response to a step input of strain ε, and $G(t)$ is a reduced relaxation function. In this study, the reduced relaxation function was approximated by a Prony series (Eq. 5) with a data analysis software (KaleidaGraph 4.0J, Synergy Software). Each of the standard deviations for reduced relaxation function showed that relaxation responses at different strain levels did not deviate much from the mean curve over the range of 8 s.

$$G(t) = 0.642e^{-t/0.0207} + 0.142e^{-t/0.482} + 0.216e^{-t/18.9} \qquad \text{(Eq. 5)}$$

According to the Quasi-LinearViscoelastic (QLV) theory [20], the stress at time t can be described by summing up contributions of all the past changes. If we approximate the elastic response σ^e described in (Eq. 4) as: $\sigma^e(\varepsilon) = A(e^{B\varepsilon} - 1)$, and assuming that the strain rate was constant during loading phase ($\varepsilon = \alpha \cdot \tau$) yields (Eq. 6),

$$\sigma(t) = \int_0^t G(t-\tau)\frac{\partial \sigma^e[\varepsilon(\tau)]}{\partial \varepsilon}\frac{\partial \varepsilon(\tau)}{\partial \tau}d\tau \qquad \text{(Eq. 6)}$$

where σ^e=0 for τ<0, and ε is the elastic nominal strain at time τ. Let $u = t-\tau$, we obtain:

$$\sigma(t) = AB\alpha\, e^{\alpha Bt} \int_0^t G(u) e^{-\alpha Bu} du \qquad \text{(Eq. 7)}$$

A and B are constants for the description of the elastic response. For the use of (Eq. 7), the coefficients A and B must be determined to describe the theoretical stress $\sigma(t)$ in (Eq. 7).

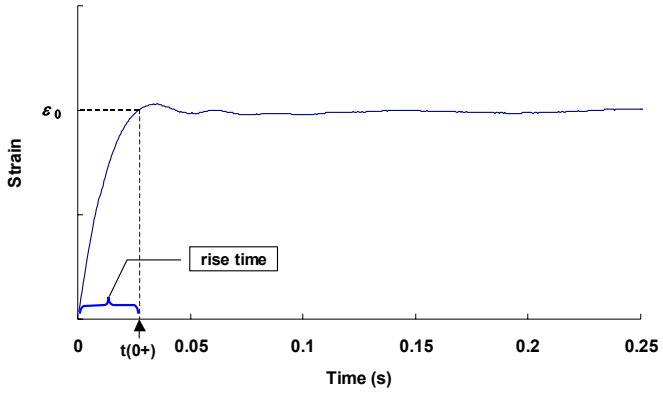

(a) Time course of the applied strain with a rise time around 30 ms.

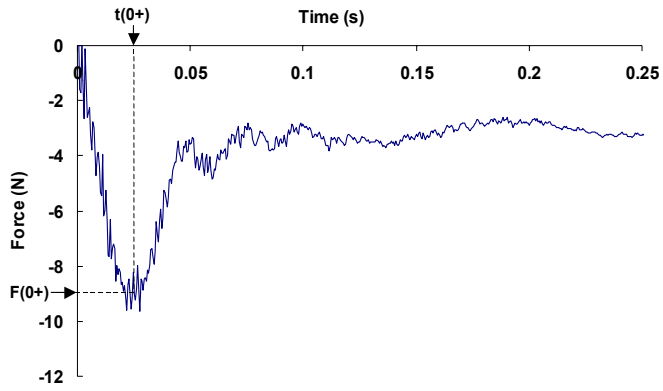

(b) Time course of the measured axial force response.

Figure 6: Typical example of a relaxation test result during initial 0.25 s.

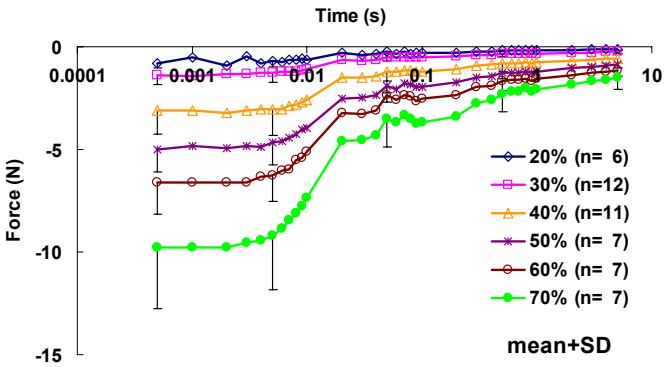

(a) Measured force responses with different compressive strains.

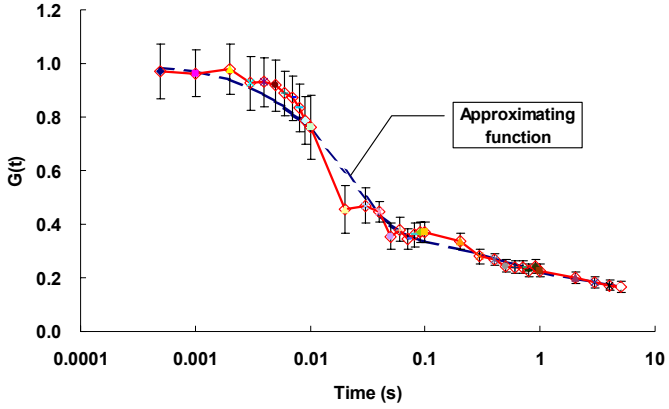

(b) Reduced relaxation function (mean±SD) approximated by a Prony series.
Figure 7: Time course of the relaxation response against a step-like strain.

4. Discussion

Understanding the biomechanics of TBIs calls for the establishment of a precise relationship between the macroscopic head motions and the mechanical response of the intracranial contents. Recently, finite element (FE) models have been used to elucidate the mechanisms of TBI. Mechanical properties of the brain employed in the computational models are crucial for predicting mechanical environments that cause TBI accurately. However, reliable data on the mechanical properties of brain tissue are still limited especially for impact simulation. To the authors' knowledge, mechanical properties under high-rate compression (>10 s^{-1}) were reported only by Estes and McElhaney [24] in the early seventies. They used fresh human and rhesus monkey brain tissues containing both white and gray matters as test model and conducted uniaxial unconfined compression test at strain rate ranging from 0.08 to 40 s^{-1} with cylindrical specimens one-half inch in diameter and one-quarter inch in height. Based on their data, Mendis et al. [25] estimated the constitutive model parameters of brain tissue and analytically obtained tangent modulus at a small nominal strain of 0.1 in uniaxial compression. The moduli were 13, 30, and 40 kPa for strain rate of 0.8, 8.0, and 40.0 s^{-1}, respectively, while the apparent elastic moduli E_1 obtained in the present study were 5.7, 11.9, and 23.8 kPa for strain rate of 1, 10, and 50 s^{-1}, respectively. The moduli obtained in their study were in the same order of magnitude as those in the present study, although they are twice higher than those obtained in the present study. The reason for the variation in the elastic moduli between the two studies is unclear at this stage, but might be ascribed to the differences in species, specimen shape, and other experimental methodology including definition of zero strain point.

Previous studies on *in vivo* animal models and *in vitro* cultured neurons exposed to injurious loading environments have suggested that the strain and strain rate associated with TBI threshold is in the range of strain exceeding ~0.2 applied at strain rates greater than 10 s^{-1} [16-18, 21]. Bayly et al. [21] experimentally verified that the strain observed during traumatic rapid indentation on *in vivo* perinatal rat brain was greater than 0.2 at strain rates greater than 40 s^{-1}. Thus, it can be said that the present approach to characterize mechanical properties of brain tissue is appropriate for understanding the mechanisms of neuronal injury in the *in vivo* brain in terms of strain and strain rate. As expected, brain tissue was noticeably rate sensitive and the averaged stress-strain relationships obtained here showed relatively stiffer responses compared to the previous results obtained under moderate loading regime [10]. Since it was impossible to produce "perfect" slip boundary at the upper and lower surfaces of the specimen during testing, we cannot ignore the possibility that our test results might have been affected by friction and the measured reaction forces were overestimated as already pointed out [22, 23]. However, the numerical study conducted by Cheng and Bilston [14], who employed poroviscoelastic model to fit the stress relaxation response of bovine white matter, indicated that, even with a friction coefficient 0.3, values of the material properties governing the viscoelasticity of the tissue

(elastic modulus and hydraulic permeability) fell within the same order of magnitude as those obtained by assuming frictionless boundary condition. On the other hand, it was also found that the rate of relaxation increased with the magnitude of the applied strain. Nevertheless, by normalizing each of the relaxation responses using each of the peak reaction forces, the present work revealed that the reduced relaxation function can be a time-dependent function while it is independent of the applied strain levels.

As previously reported by Prange and Margulies [7], it is expected that a material anisotropy weakly exists in the specimens consisted of a mixture of white (corona radiata) and gray matters. In the present study, however, we did not find significant difference stemmed from the anatomical origin or orientation of the excised test samples. The sample utilized in their study (rectangular sample: 5 mm x 10 mm with 1 mm thickness) is smaller than that used in this study (~22 mm diameter and ~14 mm height). At such relatively larger length scales, fibrous nature of the tissue would not come into play [23]. Local anisotropy and regional difference may affect stress and strain fields in impact situations, though. Donnelly and Medige [26] also reported that stress-strain relationship was not significantly dependent on the sample location within the brain or on the sample condition, in which cylindrical specimens of fresh human brain ~17 mm diameter and ~12 mm length were employed. Thereby, we assumed that brain tissue would not exhibit directional variation in mechanical properties in such a relatively large scale.

It has been reported that the neural tissue was transversely isotropic with the plane of symmetry being perpendicular to the nerve fibers [19] and stretch ratios of the nerve fibers closely correlated with their direction in the tissue [27]. In spite of their importance, the directions of nerve fibers have not been well documented yet for they are relatively complicated in cerebrum with few exceptions [28]. A detailed topography of these directions will be necessary in the future before a realistic anisotropic model of the brain can be developed.

This study might be criticized by the fact that we conducted a series of compression and relaxation tests at room temperature although, in general, most of the experimental tests using biological tissues have been performed under the well controlled constant temperature of 37°C [20]. Nonetheless, Arbogast et al. [4] did not find significant effect of temperature (5-25°C) on the viscoelastic response of brain tissue in shear. Similarly, Shen et al. [29] reported that viscoelastic response of brain tissue in the four sets of data obtained in oscillation tests under different temperatures of 37°C, 30°C, 20°C, and 10°C, collapsed on a single master curve. On the other hand, Peters et al. [30] observed the variation of the relaxation modulus with temperature in the range of 7-37°C after 10 s, which is beyond the time scale of our interest. Therefore, it is expected that the temperature difference has no influence on the normalized relaxation modulus in the range of loading regime relevant to an impact situation. Additionally, preconditioning was not performed in the current study because brain tissue does not naturally experience cyclic loading inside a cranium. On the contrary, some investigators have employed preconditioning to obtain a so-called "standardized" initial condition [5, 6, 31]. It is not clear which is the best option. At any rate, the tissue response obtained in this study exhibited reasonable consistency without preconditioning.

One of the biggest problems when working with brain tissue is degradation, which causes differences between *in vivo* and *post mortem* properties due to autolytic processes. This may change mechanical properties of animal brain as a function of time after sacrifice. Although it is inevitable, this effect was minimized by completing a series of experiments within 4 h after we obtained test specimens. In fact, McElhaney et al. [32] reported that no significant changes were found in the mechanical properties of brain tissue under *in vitro* conditions over a period of 15 h. Nicolle et al. [9] also reported that they found only a 6% increase of shear modulus between samples measured at 24 h and 48 h *post mortem*. Other problem is stemmed from the lack of active blood pressure in the vascular network. Although recent results suggested that brain properties obtained *in vitro* are relatively close to those *in situ* and *in vivo* [33], the applicability of the *in vitro* experimental results to *in vivo* environment remains unclear. Interestingly, Miller et al. [34] revealed that *in vivo* and *in vitro* mechanical properties remain within the same order of magnitude by applying *in vitro* brain tissue properties to a surgical procedure simulation. Another limitation of the present work is related to the inter-species difference between human and animal tissue

properties. It is unknown whether or not the mechanical properties of porcine brain are similar to those of human brain tissue, but Nicolle et al. [9] reported that there was no distinguishable difference existed between human and porcine brain tissues.

In this study, the long-term coefficient G_∞ representing the percentage of stress at the equilibrium state was not taken into account in the reduced relaxation function. Nonetheless, the relaxation response obtained here will be useful within the short time intervals associated with TBI and appropriate for studying an injury producing event since the relevant time period is anticipated on the order of milli-second during traumatic event. However, the responses obtained in the current study may contain some degree of relaxation because the strain input was not a true step, and the reaction force may have already relaxed during the rise time. Further research is needed to determine brain tissue constitutive models, which would enable us to incorporate the influence of the neural fiber direction as well as blood and cerebrospinal fluid pressure into the brain FE model. In the future, tensile behavior should be investigated as well under high-rate loading regime. Additionally, longer tests may be also required to more accurately determine the long-term elastic behavior of the brain tissue.

5. Conclusions

We investigated mechanical properties of porcine brain tissue under high-rate loading regime by employing unconfined compression test setup, and found that the brain tissue was noticeably rate sensitive. Additionally, we performed a series of ramp-and-hold tests and the reduced relaxation function was found to be a time-dependent function but independent of the applied strain levels in such a potentially injurious circumstances. The authors believe that these data should enhance the biofidelity of a computational model and will provide useful information relevant to the mechanisms of TBI since the accuracy in predicting the environments involved in TBI is also dependent on the biofidelity of the material properties.

References

(1) King AI, Yang KH, Zhang L, Hardy W and Viano DC, Is head injury caused by linear or angular acceleration?, In: proceedings of IRCOBI Conference (2003), pp. 1-12, Lisbon (Portugal).

(2) Tamura A, Nakahira Y, Iwamoto M, Watanabe I, Miki K, Hayashi S and Yasuki T, The influence of the traction force due to inertia of the brain mass on traumatic brain injury during SUV-to-pedestrian impact, In: proceedings of IRCOBI Conference (2006), pp. 361-364, Madrid (Spain).

(3) Fallenstein GT, Hulce VD and Melvin JW, Dynamic mechanical properties of human brain tissue, J Biomech, Vol. 2 (1969), pp. 217-226.

(4) Arbogast KB, Thibault KL, Pinheiro BS, Winey KI and Margulies SS, A high-frequency shear device for testing soft biological tissues, J Biomech, Vol. 30 (1997), pp. 757-759.

(5) Darvish KK and Crandall JR, Strain conditioning in the dynamic viscoelastic response of brain tissue, BED-Vol. 50, 2001 Bioengineering Conference ASME 2001 (2001), pp. 893-894.

(6) Bilston LE, Liu Z and Phan-Thien N, Large strain behaviour of brain tissue in shear: some experimental data and differential constitutive model, Biorheology, Vol. 38 (2001), pp. 335-345.

(7) Prange MT and Margulies SS, Regional, directional, and age-dependent properties of the brain undergoing large deformation, J Biomech Eng, Vol. 124 (2002), pp. 244-252.

(8) Brands DWA, Peters GWM and Bovendeerd PHM, Design and numerical implementation of a 3-D non-linear viscoelastic constitutive model for brain tissue during impact, J Biomech, Vol. 37 (2004), pp. 127-134.

(9) Nicolle S, Lounis M and Willinger R, Shear properties of brain tissue over a frequency range relevant for automotive impact situations: new experimental results, Stapp Car Crash J, Vol. 48 (2004), pp. 239-258.

(10) Miller K and Chinzei K, Constitutive modelling of brain tissue: experiment and theory, J Biomech, Vol. 30 (1997), pp. 1115-1121.

(11) Miller K and Chinzei K, Mechanical properties of brain tissue in tension, J Biomech, Vol.

35 (2002), pp. 483-490.

(12) Franceschini G, Bigoni D, Regitnig P and Holzapfel GA, Brain tissue deforms similarly to filled elastomers and follows consolidation theory, J Mech Phys Solids, Vol. 54 (2006), pp. 2592-2620.

(13) Velardi F, Fraternali F and Angelillo M, Anisotropic constitutive equations and experimental tensile behavior of brain tissue, Biomech Model Mechanbiol, Vol. 5 (2006), pp. 53-61.

(14) Cheng S and Bilston LE, Unconfined compression of white matter, J Biomech, Vol. 40 (2007), pp. 117-124.

(15) Kyriacou SK, Mohamed A, Miller K and Neff S, Brain mechanics for neurosurgery: modeling issues, Biomech Model Mechanobiol, Vol. 1 (2002), pp. 151-164.

(16) Bain AC and Meaney DF, Tissue-level thresholds for axonal damage in an experimental model of central nervous system white matter injury, J Biomech Eng, Vol. 122 (2000), pp. 615-622.

(17) Geddes DM and Cargill RS II, An in vitro model of neural trauma: device characterization and calcium response to mechanical stretch, J Biomech Eng, Vol. 123 (2001), pp. 247-255.

(18) Pfister BJ, Weihs TP, Betenbaugh M and Bao G, An in vitro uniaxial stretch model for axonal injury, Ann Biomed Eng, Vol. 31 (2003), pp. 589-598.

(19) Arbogast KB and Margulies SS, A fiber-reinforced composite model of the viscoelastic behavior of the brainstem in shear, J Biomech, Vol. 32 (1999), pp. 865-870.

(20) Fung YC, In: "Biomechanics: Mechanical Properties of Living Tissues Second Edition", Springer-Verlag New York Inc., New York (1993).

(21) Bayly PV, Black EE, Pedersen RC, Leister EP and Genin GM, In vivo imaging of rapid deformation and strain in an animal model of traumatic brain injury, J Biomech, Vol. 39 (2006), pp. 1086-1095.

(22) Wu JZ, Dong RG and Schopper AW, Analysis of effects of friction on the deformation behavior of soft tissues in unconfined compression tests, J Biomech, Vol. 37 (2004), pp. 147-155.

(23) Miller K, Method of testing very soft biological tissues in compression, J Biomech, Vol. 38 (2005), pp. 153-158.

(24) Estes MS and McElhaney JH, Response of brain tissue of compressive loading, In: proceedings of the 4th ASME Biomechanics Conference (1970), ASME Paper No. 70-BHF-13, pp. 1-4.

(25) Mendis KK, Stalnaker RL and Advani SH, A constitutive relationship for large deformation finite element modeling of brain tissue, J Biomech Eng, Vol. 117 (1995), pp. 279-285.

(26) Donnelly BR and Medige J, Shear properties of human brain tissue, J Biomech Eng, Vol. 119 (1997), pp. 423-432.

(27) Tamura A, Nagayama K and Matsumoto T, Measurement of nerve fiber strain in brain tissue subjected to uniaxial stretch (Comparison between local strain of nerve fiber and global strain of brain tissue), J Biomech Sci Eng, Vol. 1 (2006), pp. 304-315.

(28) Pierpaoli C and Basser PJ, Toward a quantitative assessment of diffusion anisotropy, Magn Reson Med, Vol. 36 (1996), pp. 893-906.

(29) Shen F, Tay TE, Li JZ, Nigen S, Lee PVS and Chan HK, Modified Bilston nonlinear viscoelastic model for finite element head injury studies, J Biomech Eng, Vol. 128 (2006), pp. 797-801.

(30) Peters GWM, Meulman JH and Sauren AAH, The applicability of the time/temperature superposition principle to brain tissue, Biorheology, Vol. 34 (1997), pp. 127-138.

(31) Hrapko M, van Dommelen JAW, Peters GWM and Wismans JSHM, The mechanical behaviour of brain tissue: large strain response and constitutive modelling, In: proceedings of IRCOBI Conference (2005), pp. 59-69, Prague (Czech).

(32) McElhaney JH, Melvin JW, Roberts VL and Portnoy HD, Dynamic characteristics of the tissues of the head, In: Perspectives in Biomedical Engineering (Kenedi RM eds.), University Park Press, Baltimore, (1973), pp. 215-222.

(33) Gefen A and Margulies SS, Are in vivo and in situ brain tissues mechanically similar?, J Biomech, Vol. 37 (2004), pp. 1339-1352.

(34) Miller K, Chinzei K, Orssengo G and Bednarz P, Mechanical properties of brain tissue in-vivo: experiment and computer simulation, J Biomech, Vol. 33 (2000), pp. 1369-1376.